Electrons on hexagonal lattices and applications to nanotubes

Betti Hartmann* and Wojtek J. Zakrzewski[†]

Department of Mathematical Sciences, University of Durham, Durham DH1 3LE, United Kingdom
(Received 8 April 2003; revised manuscript received 13 May 2003; published 12 November 2003)

We consider a Fröhlich-type Hamiltonian on a hexagonal lattice. Aiming to describe nanotubes, we choose this two-dimensional lattice to be periodic and to have a large extension in one (x) direction and a small extension in the other (y) direction. We study the existence of solitons in this model using both analytical and numerical methods. We find exact solutions of our equations and discuss some of their properties.

I. INTRODUCTION

Nanotubes have attracted a large amount of interest ever since they were first discovered in 1991.[1] They can be thought of as carbon cylinders with a hexagonal grid and are thus fullerene related structures. Their mechanical, thermal, optical, and electrical properties have been studied in some detail.[2] It was found that most properties depend crucially on the diameter, chirality, and length of the tube. A distortion of the lattice thus affects the energy-band gap. This distortion of the lattice can be achieved in two different ways: (a) through an external force such as, e.g., bending, stretching, or twisting[3] or (b) through an internal excitation, which interacts with the lattice. It is well known that the interaction of an excitation such as an amide I vibration in biopolymers or an electron (in the case of the Fröhlich Hamiltonian) with a lattice whose distortion is initially caused by the excitation results in the creation of a localized state which, in what follows, we refer to as a soliton. Such a soliton was first introduced by Davydov[4] in 1970s to explain the dispersion-free energy transport in biopolymers (see also Ref. 5 for further details).

Recently, a Fröhlich Hamiltonian was studied on a two-dimensional, discrete, quadratic lattice.[6–8] In Refs. 6 and 7, the existence of localized states was studied numerically and it was found that their properties depend crucially on the electron-phonon coupling constant. An analytical study confirmed these results[8] by showing that in the continuum limit the set of discrete equations reduces to a modified nonlinear Schrödinger (MNLS) equation which has an additional term resulting from the discreteness of the lattice. Although a soliton of the basic NLS is unstable the extra term was shown to stabilize it for appropriate choices of the coupling constant.

In this paper, we extend the study of Refs. 6–8 to the case of a hexagonal, periodic lattice with a large extension in x and a small extension in y directions. We study the resultant equations both analytically and numerically. In Sec. II, we present the Hamiltonian and the equations of motion. In Sec. III, we discuss various properties of the equations in the stationary limit and demonstrate the existence of an exact solution of the discrete equations. In this limit, we can thus replace the full system of equations by a modified discrete nonlinear Schrödinger (DNLS) equation. In Sec. IV, we present and compare our numerical results for the continuous MNLS equation, for the full system of equations, and for the modified DNLS equation. Most of our numerical simulations are performed for the (5,5) armchair tube. Such nanotube was discussed in a recent paper by Liu *et al.* in the context of nanorings.[9] We also discuss briefly how nanotubes with different diameter and chirality could be constructed in our model.

II. THE HAMILTONIAN AND EQUATIONS OF MOTION

A. Hamiltonian

The Hamiltonian H of our model is a sum of four sums which result from the special features of the hexagonal grid. $\psi_{i,j}$ denotes the electron field on the ith and the jth lattice side, while $u_{i,j}$ and $v_{i,j}$ are the displacements of the ith and the jth lattice point from equilibrium in the x and y directions, respectively:

$$
H = \sum_{(j-1)/2=0}^{(N_2/2)-1} \sum_{(i-1)/4=0}^{(N_1/4)-3} \left[(E+W)\psi_{i,j}\psi_{i,j}^* - j_x\psi_{i,j}^*(\psi_{i+1,j+1}+\psi_{i-1,j}+\psi_{i+1,j-1}) - j_x\psi_{i,j}(\psi_{i+1,j+1}^*+\psi_{i-1,j}^*+\psi_{i+1,j-1}^*) \right.
$$

$$
\left. + |\psi_{i,j}|^2 \left(\frac{c_x}{3}(u_{i+1,j+1}+u_{i+1,j-1}-2u_{i-1,j}) + \frac{c_x}{\sqrt{3}}(v_{i+1,j+1}-v_{i+1,j-1}) \right) \right] + \sum_{j/2=1}^{N_2/2} \sum_{(i-2)/4=0}^{(N_1/4)-2} \left[(E+W)\psi_{i,j}\psi_{i,j}^* \right.
$$

$$
- j_x\psi_{i,j}^*(\psi_{i+1,j}+\psi_{i-1,j+1}+\psi_{i-1,j-1}) - j_x\psi_{i,j}(\psi_{i+1,j}^*+\psi_{i-1,j+1}^*+\psi_{i-1,j-1}^*) + |\psi_{i,j}|^2
$$

$$
\left. \times \left(\frac{c_x}{3}(-u_{i-1,j-1}-u_{i-1,j+1}+2u_{i+1,j}) + \frac{c_x}{\sqrt{3}}(v_{i-1,j+1}-v_{i-1,j-1}) \right) \right]
$$

$$+ \sum_{j/2=1}^{N_2/2} \sum_{(i-3)/4=0}^{(N_1/4)-1} \left[(E+W)\psi_{i,j}\psi_{i,j}^* - j_x\psi_{i,j}^*(\psi_{i+1,j+1}+\psi_{i-1,j}+\psi_{i+1,j-1}) - j_x\psi_{i,j}(\psi_{i+1,j+1}^*+\psi_{i-1,j}^*+\psi_{i+1,j-1}^*) \right.$$

$$\left. + |\psi_{i,j}|^2 \left(\frac{c_x}{3}(u_{i+1,j+1}+u_{i+1,j-1}-2u_{i-1,j}) + \frac{c_x}{\sqrt{3}}(v_{i+1,j+1}-v_{i+1,j-1}) \right) \right]$$

$$+ \sum_{(j-1)/2=0}^{(N_2/2)-1} \sum_{i/4=1}^{N_1/4} \left[(E+W)\psi_{i,j}\psi_{i,j}^* - j_x\psi_{i,j}^*(\psi_{i+1,j}+\psi_{i-1,j+1}+\psi_{i-1,j-1}) - j_x\psi_{i,j}(\psi_{i+1,j}^*+\psi_{i-1,j+1}^*+\psi_{i-1,j-1}^*) \right.$$

$$\left. + |\psi_{i,j}|^2 \left(\frac{c_x}{3}(-u_{i-1,j-1}-u_{i-1,j+1}+2u_{i+1,j}) + \frac{c_x}{\sqrt{3}}(v_{i-1,j+1}-v_{i-1,j-1}) \right) \right] \tag{1}$$

with phonon energy W,

$$W = \frac{1}{2}M\sum_{j=1}^{N_2}\sum_{i=1}^{N_1}\left(\left(\frac{du_{ij}}{dt}\right)^2 + \left(\frac{dv_{ij}}{dt}\right)^2 \right) + \frac{1}{2}M\sum_{(j-1)/2=0}^{(N_2/2)-1}\sum_{(i-1)/4=0}^{(N_1/4)-3} (k_x[(u_{ij}-u_{i-1,j})^2 + (v_{ij}-v_{i-1,j})^2 + (u_{ij}-u_{i+1,j+1})^2$$

$$+ (v_{ij}-v_{i+1,j+1})^2 + (u_{ij}-u_{i+1,j-1})^2 + (v_{ij}-v_{i+1,j-1})^2]) + \frac{1}{2}M\sum_{j/2=1}^{N_2/2}\sum_{(i-2)/4=0}^{(N_1/4)-2} (k_x[(u_{ij}-u_{i+1,j})^2 + (v_{ij}-v_{i+1,j})^2$$

$$+ (u_{ij}-u_{i-1,j+1})^2 + (v_{ij}-v_{i-1,j+1})^2 + (u_{ij}-u_{i-1,j-1})^2 + (v_{ij}-v_{i-1,j-1})^2]) + \frac{1}{2}M\sum_{j/2=1}^{N_2/2}\sum_{(i-3)/4=0}^{(N_1/4)-1} (k_x[(u_{ij}-u_{i-1,j})^2$$

$$+ (v_{ij}-v_{i-1,j})^2 + (u_{ij}-u_{i+1,j+1})^2 + (v_{ij}-v_{i+1,j+1})^2 + (u_{ij}-u_{i+1,j-1})^2 + (v_{ij}-v_{i+1,j-1})^2])$$

$$+ \frac{1}{2}M\sum_{(j-1)/2=0}^{(N_2/2)-1}\sum_{i/4=1}^{N_1/4} (k_x[(u_{ij}-u_{i+1,j})^2 + (v_{ij}-v_{i+1,j})^2 + (u_{ij}-u_{i-1,j+1})^2 + (v_{ij}-v_{i-1,j+1})^2$$

$$+ (u_{ij}-u_{i-1,j-1})^2 + (v_{ij}-v_{i-1,j-1})^2]). \tag{2}$$

j_x is the electron field self-interaction coupling, c_x couples the electron field to the displacement fields u and v, and k_x is the self-coupling of the displacement fields.

B. Equations of motion

We can easily derive the equations of motion from our Hamiltonian H. As an example, we give the equations for $i = 1+4k$. The discrete Schrödinger equation for the $\psi_{i,j}$ field thus becomes

$$i\hbar \frac{\partial \psi_{i,j}}{\partial t} = (E+W)\psi_{i,j} - 2j_x(\psi_{i+1,j+1}+\psi_{i-1,j}+\psi_{i+1,j-1})$$

$$+ \psi_{i,j}\left[\frac{c_x}{3}(u_{i+1,j+1}+u_{i+1,j-1}-2u_{i-1,j}) \right.$$

$$\left. + \frac{c_x}{\sqrt{3}}(v_{i+1,j+1}-v_{i+1,j-1}) \right], \tag{3}$$

while the equations for the displacement fields $u_{i,j}$ and $v_{i,j}$ are given by

$$\frac{d^2u_{i,j}}{dt^2} = k_x(3u_{i,j}-u_{i+1,j+1}-u_{i-1,j}-u_{i+1,j-1})$$

$$+ \frac{c_x}{3M}(2|\psi_{i-1,j}|^2-|\psi_{i+1,j+1}|^2-|\psi_{i+1,j-1}|^2), \tag{4}$$

and

$$\frac{d^2v_{i,j}}{dt^2} = k_x(3v_{i,j}-v_{i+1,j+1}-v_{i-1,j}-v_{i+1,j-1})$$

$$- \frac{c_x}{\sqrt{3}M}(|\psi_{i+1,j+1}|^2-|\psi_{i+1,j-1}|^2). \tag{5}$$

We perform the following rescalings:

$$\tau = \frac{j_x t}{\hbar}, \quad U=3C_x u, \quad V=3C_x v, \quad E_0=\frac{E}{j_x}, \quad W_0=\frac{W}{j_x} \tag{6}$$

and introduce the following rescaled coupling constants:

$$C_x = \frac{c_x}{9j_x}, \quad K_x = \frac{k_x \hbar^2}{j_x^2}, \quad g = \frac{2C_x^2}{E_s}, \quad E_s = \frac{Mj_x}{9\hbar^2}. \quad (7)$$

The equations then read

$$i\frac{\partial \psi_{i,j}}{\partial \tau} = (E_0 + W_0)\psi_{i,j} - 2(\psi_{i+1,j+1} + \psi_{i-1,j} + \psi_{i+1,j-1})$$

$$+ \psi_{i,j}[(U_{i+1,j+1} + U_{i+1,j-1} - 2U_{i-1,j})$$

$$+ \sqrt{3}(V_{i+1,j+1} - V_{i+1,j-1})], \quad (8)$$

$$\frac{d^2 U_{i,j}}{d\tau^2} = K_x(3U_{i,j} - U_{i+1,j+1} - U_{i-1,j} - U_{i+1,j-1})$$

$$+ \frac{g}{2}(2|\psi_{i-1,j}|^2 - |\psi_{i+1,j+1}|^2 - |\psi_{i+1,j-1}|^2), \quad (9)$$

and

$$\frac{d^2 V_{i,j}}{d\tau^2} = K_x(3V_{i,j} - V_{i+1,j+1} - V_{i-1,j} - V_{i+1,j-1})$$

$$- \frac{\sqrt{3}g}{2}(|\psi_{i+1,j+1}|^2 - |\psi_{i+1,j-1}|^2). \quad (10)$$

III. STATIONARY LIMIT

In the stationary limit, we have

$$\lambda\psi_{i,j} + 2(3\psi_{i,j} - \psi_{i+1,j+1} - \psi_{i-1,j} - \psi_{i+1,j-1})$$

$$+ \psi_{i,j}[U_{i+1,j+1} + U_{i+1,j-1} - 2U_{i-1,j}$$

$$+ \sqrt{3}(V_{i+1,j+1} - V_{i+1,j-1})]$$

$$= 0, \quad (11)$$

where $\lambda = E_0 + W_0 - 6$ and

$$3U_{i,j} - U_{i+1,j+1} - U_{i-1,j} - U_{i+1,j-1}$$

$$= -\frac{\tilde{g}}{2}(2|\psi_{i-1,j}|^2 - |\psi_{i+1,j+1}|^2 - |\psi_{i+1,j-1}|^2), \quad (12)$$

$$3V_{i,j} - V_{i+1,j+1} - V_{i-1,j} - V_{i+1,j-1}$$

$$= \frac{\sqrt{3}\tilde{g}}{2}(|\psi_{i+1,j+1}|^2 - |\psi_{i+1,j-1}|^2), \quad (13)$$

where $\tilde{g} = g/K_x$.

A. Discrete equation

In contrast to the square grid, we find that the discrete equations of the hexagonal grid in the stationary limit do have an *exact* solution. We can thus replace the system of

coupled equations (3)–(5) by just one modified DNLS equation. We again look at the case $i = 1 + 4k$ for which we have

$$\Delta(1)U_{ij} = \frac{\tilde{g}}{2}(2|\psi_{i-1,j}|^2 - |\psi_{i+1,j+1}|^2 - |\psi_{i+1,j-1}|^2),$$

where $\Delta(1)U_{ij} = U_{i+1,j+1} + U_{i-1,j} + U_{i+1,j-1} - 3U_{i,j}$. Analogously, we have

$$\Delta(1)V_{ij} = \frac{\sqrt{3}\tilde{g}}{2}(|\psi_{i+1,j-1}|^2 - |\psi_{i+1,j+1}|^2),$$

where $\Delta(1)V_{ij} = V_{i+1,j+1} + V_{i-1,j} + V_{i+1,j-1} - 3V_{i,j}$. Next we note that for the three nearest neighbors we have similar relations, namely,

$$\Delta(1)U_{i+1,j+1} = \frac{\tilde{g}}{2}(|\psi_{i,j}|^2 + |\psi_{i,j+2}|^2 - 2|\psi_{i+2,j+1}|^2),$$

$$\Delta(1)U_{i+1,j-1} = \frac{\tilde{g}}{2}(|\psi_{i,j-2}|^2 + |\psi_{i,j}|^2 - 2|\psi_{i+2,j-1}|^2),$$

$$\Delta(1)U_{i-1,j} = \frac{\tilde{g}}{2}(|\psi_{i-2,j-1}|^2 + |\psi_{i-2,j+1}|^2 - 2|\psi_{i,j}|^2)$$

for the U field and

$$\Delta(1)V_{i+1,j+1} = \frac{\sqrt{3}\tilde{g}}{2}(|\psi_{ij}|^2 - |\psi_{i,j+2}|^2),$$

$$\Delta(1)V_{i+1,j-1} = \frac{\sqrt{3}\tilde{g}}{2}(|\psi_{i,j-2}|^2 - |\psi_{ij}|^2)$$

for the V field.
Defining

$$Z_a = U_{i+1,j+1} + U_{i+1,j-1} - 2U_{i-1,j}$$

$$+ \sqrt{3}(V_{i+1,j+1} - V_{i+1,j-1})$$

[i.e., the lattice terms in Eq. (11)] we find that the following discrete equation holds:

$$\Delta(1)Z_a = \tilde{g}(6|\psi_{ij}|^2 - |\psi_{i,j+2}|^2 - |\psi_{i+2,j+1}|^2 - |\psi_{i,j-2}|^2$$

$$- |\psi_{i+2,j-1}|^2 - |\psi_{i-2,j-1}|^2 - |\psi_{i-2,j+1}|^2).$$

The right-hand side of Eq. (14) is a seven-point Laplacian $\Delta(2)|\psi_{ij}|^2$, thus we find

$$\Delta(1)Z_a = -\tilde{g}\Delta(2)|\psi_{ij}|^2. \quad (14)$$

It is easy to see that one possible solution of this equation is of the form

$$Z_a = -\tilde{g}(|\psi_{i+1,j+1}|^2 + |\psi_{i+1,j-1}|^2 + |\psi_{i-1,j}|^2 + 3|\psi_{ij}|^2). \quad (15)$$

This is quite remarkable since on a square lattice a similar equation has no simple solution. Inserting Eq. (15) into Eq. (11) we have

$$\lambda \psi_{i,j} + 2(3\psi_{i,j} - \psi_{i+1,j+1} - \psi_{i-1,j} - \psi_{i+1,j-1})$$
$$- \widetilde{g}\psi_{i,j}[|\psi_{i+1,j+1}|^2 + |\psi_{i+1,j-1}|^2 + |\psi_{i-1,j}|^2 + 3|\psi_{ij}|^2]$$
$$= 0$$

or

$$\lambda \psi_{i,j} - 2\Delta(1)\psi_{ij} - \widetilde{g}\psi_{i,j}(\Delta(1)|\psi_{i,j}|^2 + 6|\psi_{ij}|^2) = 0. \tag{16}$$

This equation constitutes our DNLS equation.

B. Continuum limit

Next we look at the continuum limit of Eq. (16). To do this we introduce the following expansions:

$$\psi_{i\pm1,j+1} = \psi \pm \delta x_\pm \frac{\partial \psi}{\partial x} + \delta y \frac{\partial \psi}{\partial y} + \frac{1}{2}(\delta x_\pm)^2 \frac{\partial^2 \psi}{\partial x^2}$$

$$\pm \delta y \, \delta x_\pm \frac{\partial^2 \psi}{\partial x \partial y} + \frac{1}{2}(\delta y)^2 \frac{\partial^2 \psi}{\partial y^2} \pm \frac{1}{8}(\delta x_\pm)^3 \frac{\partial^3 \psi}{\partial x^3}$$

$$+ \frac{1}{2}(\delta x_\pm)^2 \delta y \frac{\partial^3 \psi}{\partial x^2 \partial y} \pm \frac{1}{2} \delta x_\pm (\delta y)^2 \frac{\partial^3 \psi}{\partial x \partial y^2}$$

$$+ \frac{1}{8}(\delta y_\pm)^3 \frac{\partial^3 \psi}{\partial y^3} \pm \cdots \tag{17}$$

and

$$\psi_{i\pm1,j-1} = \psi \pm \delta x_\pm \frac{\partial \psi}{\partial x} - \delta y \frac{\partial \psi}{\partial y} + \frac{1}{2}(\delta x_\pm)^2 \frac{\partial^2 \psi}{\partial x^2}$$

$$\mp \delta y \, \delta x_\pm \frac{\partial^2 \psi}{\partial x \partial y} + \frac{1}{2}(\delta y)^2 \frac{\partial^2 \psi}{\partial y^2} \pm \frac{1}{8}(\delta x_\pm)^3 \frac{\partial^3 \psi}{\partial x^3}$$

$$- \frac{1}{2}(\delta x_\pm)^2 \delta y \frac{\partial^3 \psi}{\partial x^2 \partial y} \pm \frac{1}{2} \delta x_\pm (\delta y)^2 \frac{\partial^3 \psi}{\partial x \partial y^2}$$

$$- \frac{1}{8}(\delta y_\pm)^3 \frac{\partial^3 \psi}{\partial y^3} \pm \cdots, \tag{18}$$

where for $i = 1 + 4k$ and $i = 3 + 4k$ we have $\delta x_+ = 1/2$, $\delta x_- = 1$, while for $i = 2 + 4k$ and $i = 4 + 4k$ we have $\delta x_+ = 1$, $\delta x_- = 1/2$. Moreover, $\delta y = \sqrt{3}/2$. Inserting this into Eq. (16), we obtain

$$\lambda \psi - \frac{3}{2}\Delta \psi - \widetilde{g}\psi\left(\frac{3}{4}\Delta|\psi|^2 + 6|\psi|^2\right) = 0 \tag{19}$$

or, equivalently,

$$\widetilde{\lambda}\psi + \Delta\psi + 4\widetilde{g}\psi\left(|\psi|^2 + \frac{1}{8}\Delta|\psi|^2\right) = 0. \tag{20}$$

We thus have, in analogy to what was found in Refs. 6–8, the MNLS equation with an extra term, which can stabilize the soliton:

$$i\frac{\partial \psi}{\partial \tau} + \Delta\psi + 4\widetilde{g}\psi\left(|\psi|^2 + \frac{1}{8}\Delta|\psi|^2\right) = 0. \tag{21}$$

Following Refs. 6–8 we see that the conserved energy in this case is given by

$$\mathcal{E} = \int \left(|\vec{\nabla}\psi|^2 - 2\widetilde{g}|\psi|^4 + \frac{\widetilde{g}}{4}(\vec{\nabla}|\psi|^2)^2\right) dx \, dy. \tag{22}$$

Approximating the soliton solution of Eq. (21) by a Gaussian of the form $\psi(x,y) = \kappa/\sqrt{\pi}\exp(-\kappa^2/2(x^2 + y^2))$ we find that the value of κ that minimizes the energy is

$$\kappa_{min}^2 = 2\left(1 - \frac{\pi}{\widetilde{g}}\right) \tag{23}$$

and thus we have an estimate of the critical $\widetilde{g}$, namely, $\widetilde{g}_{cr} \sim \pi$.

IV. NUMERICAL RESULTS

A. Continuous, modified nonlinear Schrödinger equation

First, we have considered the continuous, modified nonlinear Schrödinger equation (21). For this, we have taken the radially symmetric ansatz

$$\psi(r,t) = e^{i\alpha t}R(r), \tag{24}$$

and put this into Eq. (21). Then we have solved the ordinary differential equation (ODE) using a collocation method for the boundary value ODEs[10] and choosing the boundary conditions:

$$\frac{\partial R(r)}{\partial r}\Big|_{r=0} = 0, \quad R(r=\infty) = 0. \tag{25}$$

Our results are shown in Fig. 1. For a fixed $\widetilde{g}$ we have determined the value of the function $R(r)$ at the origin, $R(r=0)$, as well as the value of α for which the norm of the solution is equal to unity. As can be seen from Fig. 1, we have found that for a critical value of $\widetilde{g} = \widetilde{g}_{cr} \approx 2.94$ the value of $R(0)$ tends to zero. Since our construction is such that the maximum of the solution is located at $r = 0$, the value of the height of the solution tends to zero and thus the solution ceases to exist. We thus find that the critical value of $\widetilde{g}$ from our numerical construction agrees with the upper-bound value obtained from the variational approach based on the Gaussian, namely, $\widetilde{g}_{cr} = \pi$.

Note that the solutions cease to exist when the value of α tends to zero. Since we can interpret α as the frequency of an internal rotation, the solutions apparently cease to exist when there is no internal rotation. This can be compared to the so-called "Q-balls" which are nontopological solitons characterized also by a complex scalar field[11] of the form similar to Eq. (24). For them it is known[11] that there exist upper and lower positive-valued bounds on the frequency of the internal rotation in order for Q-balls to be stable. In comparison, our solutions exist for all values of $\alpha > 0$. This is probably due to the fact that while the dynamical part of our action is
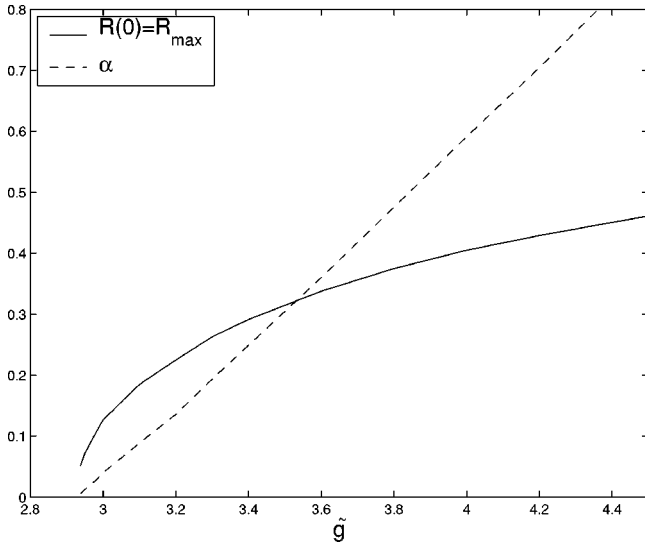
FIG. 1. The results obtained with the ansatz $\psi(r,\theta) = e^{i\alpha t} R(r)$ to solve the continuous modified NLS equation. In this figure, the value of the function $R(r)$ at the origin $R(0)$, which in our construction is equal to the maximum of R, R_{max} is shown as function of $\tilde{g}$. The values of α are also shown. The solutions shown have normal one.

similar to that for Q-balls, we have an extra term involving derivatives as compared to an "ordinary" ψ^6-potential in the case of Q-balls.

B. Discrete equations

1. Full system of equations

For our numerical study of the full equations (3)–(5) we have found it convenient to "squeeze" the lattice as indicated in Figs. 2(a) and 2(b). The Hamiltonian and the corresponding equations are given in the Appendix. For our numerical calculations, we have used mainly a periodic grid with $N_1 = 160$ and $N_2 = 20$. We have in addition chosen the boundary conditions such that the fields at $(i=0,j)$ are identified with those at $(i=i_{max},j)$. Thus the type of nanotube we are studying here is a (5,5) armchair tube which is metallic.[2] Nanotubes can also be semiconducting and we make a brief comment about the possibility of constructing semiconducting tubes in our model in the last paragraph of this section.

In this work, the C—C bond length, 0.1415 nm,[12] is normalized to unity. Therefore, the tube diameter is 0.6756 nm. Tubes with different diameter can also be constructed in our model. We discuss this together with different chiralities in the last paragraph of this section.

As starting configuration we have used an exponential-like excitation $\psi_{i,j}$ extended typically over the lattice points $i=78$–83 and $j=3$–7 with the lattice at equilibrium everywhere, i.e., $u_{i,j}=0$ and $v_{i,j}=0$ for all i,j. We are mainly interested in the existence of solitons and their dependence on the value of the coupling constant c_x. We have set $j_x = k_x = 1$, $M = 20$, and $E = 0.142\,312$. The main goal of this
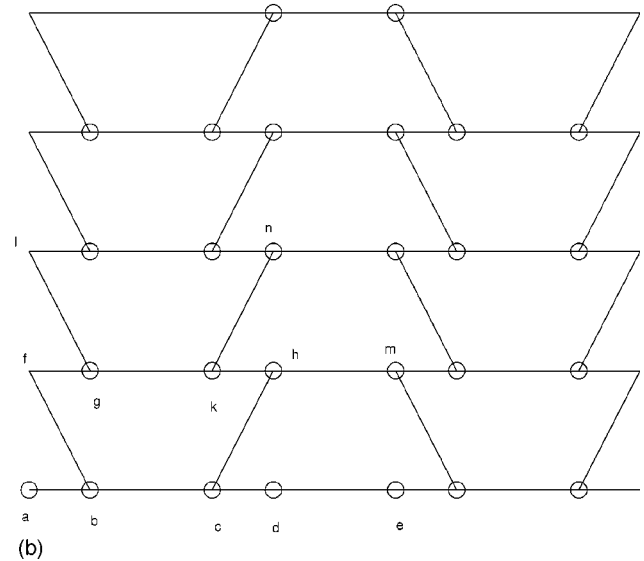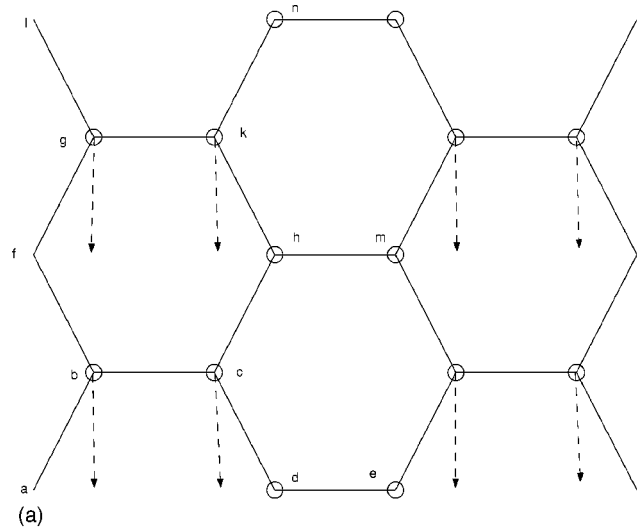

FIG. 2. (a) The hexagonal lattice is shown. The arrows indicate the method of "squeezing" the lattice for the numerical evaluation. (b) The "squeezed" hexagonal lattice for the numerical construction. The Hamiltonian H^n corresponding to this lattice is given in the Appendix of the paper.

work is to study the dependence on c_x. So the exact values of j_x and k_x play a minor role. Hence, we have set them to one. The choice of $M = 20$ is a reflection of the physical fact that the mass of the carbon atom is $\approx 20 \times 10^{-24} g$.

To absorb the energy thus allowing the initial configuration to evolve into the stationary solutions of Eqs. (3)–(5), i.e., of Eqs. (11)–(13) we have additionally introduced damping terms $\nu(du_{i,j}/dt)$ and $\nu(dv_{i,j}/dt)$, respectively, into Eqs. (4) and (5). We have typically chosen $\nu = 0.25$ -0.75. For this choice of the coupling constants, we have performed several numerical calculations using a fourth-order Runge-Kutta method for simulating the time evolution. We have found that solitons exist in this system for $c_x > \approx 20$. For larger values of c_x, the soliton forms very quickly, while decreasing c_x the time increases at which a
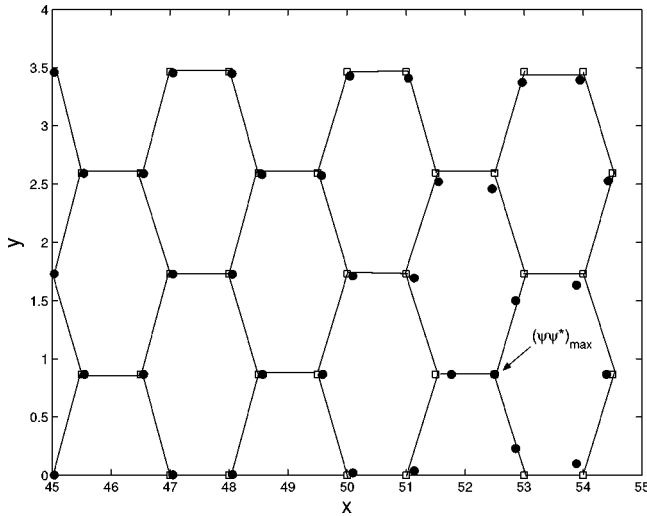
FIG. 3. The distortion of the lattice close to the location of the soliton is shown. The squares indicate the undistorted lattice, while the circles indicate the distorted lattice after $t=4000$; $c_x=25$. The corresponding soliton's maximum $(\psi\psi^*)_{max}\approx 0.6145$.

FIG. 4. The height of the soliton's maximum $(\psi_{i,j}\psi_{i,j}^*)_{max}$ is shown as a function of the parameter $\tilde{g}$.

soliton forms. This is of course due to the weaker coupling between the dynamics of the lattice itself and the excitation. For $c_x=19$, we have waited until $t\approx 8000$ and have not found a soliton. Moreover, in all cases we have found only little displacement of the lattice from the equilibrium. We have found that at the location of the soliton the lattice becomes squeezed (i.e., the lattice sites move towards the sites at which the soliton is located). This is demonstrated in Fig. 3 for $c_x=25$, where we show the lattice distortion after $t=4000$. The point at which the center of the soliton is located does not move, while the sites in its close neighborhood all move towards the center of the soliton.

We have also studied the effects of perturbations of the solitons. We have found that after perturbing the soliton we obtain a new solution with a different height of the soliton maximum. Even after introducing a perturbation which keeps the maximal height fixed, the new solution differs from the starting one. We thus come to the conclusion that the full system of Eqs. (3)–(5) has a large number of solutions for each choice of coupling constants. We believe that a conserved quantity exists in this system which picks out the specific solution. However, so far we have not been able to determine this conserved quantity.

2. Modified, discrete nonlinear Schrödinger equation

In addition to the full system of equations, we have also studied the dynamical analog of Eq. (16). Using a similar starting configuration with $\psi_{i,j}$ being exponential and non-zero over $i=78$–83 and $j=3$–7, we have determined the value of $\tilde{g}$ for which a soliton exists. Our results are shown in Fig. 4, where we present the height of the soliton's maximum $(\psi\psi^*)_{max}$ as function of $\tilde{g}$. We find that the value of $\tilde{g}$ at which the soliton disappears $\tilde{g}_{cr}\approx 2.295$. The height of the soliton at this critical coupling is $(\psi_{i,j}\psi_{i,j}^*)_{max}\approx 0.227$. Our numerical study of the continuous MNLS equation gave us
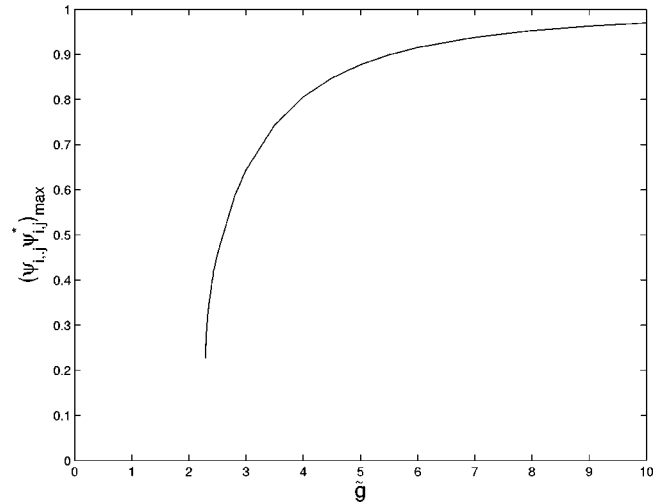
$\tilde{g}_{cr}\approx 2.94$, while the analytical study led to $\tilde{g}_{cr}=\pi$. Both values are not a bad approximation for the value found numerically for the discrete equation.

To test the independence of our results from the form of the initial settings, we have used a different starting configuration with two exponential-like excitations being located at $i=78$–83, $j=3$–7 and $i=138$–143 and $j=13$–17, respectively. We have found that for values $\tilde{g}>\approx 3$, the results agree. For both types of initial configurations, the minimal energy configuration corresponds to one soliton. However, having said this, the time to reach this minimal energy configurations is significantly smaller for the initial configuration with one excitation than for that with two excitation (typically one order of magnitude smaller). We have also tested our results as to the dependence on the size of the grid. For this, we have chosen two excitations on three different grid sizes: (a) a grid with $N_1=160$, $N_2=20$, and two exponential excitations extended over $i=78$–83, $j=3$–7 and $i=138$–143, $j=13$–17, respectively, (b) a grid with $N_1=320$ and $N_2=40$ with the excitations located at the same places as in (a), and finally (c) a grid with $N_1=60$, $N_2=10$, and two exponential excitations extended over $i=18$–23, $j=2$–4 and $i=38$–43, $j=7$–9, respectively. We have found that for $\tilde{g}=3$, the results of cases (a) and (c) agree. For the case (a) the soliton forms at $t\approx 300$, while for the case (c) it forms at $t\approx 100$. This is not surprising since in the case (c), the two excitations are located nearer to each other than in the case (a). To test the dependence on the actual lattice size we have compared the cases (a) and (b). We have found that the larger the lattice the longer it takes for the soliton to form. For $\tilde{g}=3$ a soliton forms after $t\approx 300$ in the case (a), while for (b) it forms at $t>700$. We have thus found that, in comparison with the case of the full system of equations, the solutions of the DNLS equation are unique for each choice of the coupling constant.

3. Comparison of results

Since we have found that in the stationary limit the full system of equations can be replaced by the DNLS equation, the minimal energy solutions we have obtained for both types of equations should be in agreement.

Comparing the two systems, we see that the value $\tilde{g}$ is given in terms of the coupling constants of the full system by

$$\tilde{g} = \frac{2}{9} \frac{c_x^2}{M j_x k_x}, \tag{26}$$

which, for the choice of coupling constants we have used in our numerical simulations, gives

$$\tilde{g} = \frac{c_x^2}{90}. \tag{27}$$

Thus a critical value of $c_x \approx 20$ would imply $\tilde{g}_{cr} \approx 4.4$. First, we remark that the values of the critical electron-phonon coupling we obtained from all our simulations (including those for the continuous MNLS equation) are of the same order of magnitude. However, there is a slight discrepancy between the results for the full system and the DNLS equation. We believe that this is due to the fact that there might exist additional terms $\mathcal{A}$ in Eq. (15) for which $\Delta(1)\mathcal{A}=0$ and/or $\Delta(2)\mathcal{A}=0$. These terms would then appear in Eq. (16) and would change the comparison of the solutions. However, it is difficult to determine these additional terms and so this is left as a future work.[13]

4. Tubes with different diameter, chirality, and lengths

Since most of our results are for a (5,5) armchair tube and since it is well known that the properties of nanotubes depend strongly on the diameter, chirality, and lengths of the tube, we will discuss briefly how different tubes could be constructed in our model. We have not constructed these tubes yet, but we aim to do so in a future publication in which we intend to extend our approach to a more realistic three-dimensional model.[13]

Labeling the first carbon atom in the y direction by $j=0$, we have chosen j_{max} such that it is divisible by 4. Thus, the length of the tube in the y direction is $l_y = \frac{3}{4} j_{max}$. Since we identify the fields labeled by $(i=0,j)$ with those at $(i=i_{max},j)$, the diameter of the tube is given by $d = l_y/\pi$. Thus increasing/decreasing j_{max} by $4n$, $n=1,2,3,\dots$, we can construct armchair nanotubes with diameters $d=(3/4\pi)(j_{max}\pm 4n)$. Similarly, we can construct longer tubes by increasing the number of atoms in the x direction.

As far as chirality is concerned, there are two things to modify in our model in order to be able to construct tubes with different chirality. One is to change the number of points in the y direction so that j_{max} is nondivisible by 4. The other is to adjust the periodic boundary conditions in the y direction appropriately. If we, e.g., choose $j_{max}=18$, we have to identify the fields at $(i=0,j)$ with those at $(i=i_{max},j+1)$. This then would give us a (5,4) nanotube

which would be semiconducting.

In this work, we have concentrated our attention on the existence of localized structures. These structures extend over large parts of our grids, but are negligible at boundaries. Hence, we expect these to hold for systems with different boundary conditions, i.e., different chiralities.

V. CONCLUSIONS

Motivated by a large amount of research done in the area of nanotubes, we have studied solitons on a two-dimensional hexagonal lattice. We have chosen our lattice to be periodic in both the x and y directions and to be of large extension in one (x) direction and of small extension in the other (y) direction. In the stationary limit, we have found that the full system of equations in which the electron excitation is coupled to the displacement fields of the lattice can be replaced by a modified discrete nonlinear Schrödinger (DNLS) equation. This discovery of an exact solution of the full system of equations is remarkable since for the similar quadratic lattice such a simple solution does not exist.

In our numerical studies we have mainly concentrated our attention on determining the value of the critical phonon-electron coupling constant. For the DNLS we have found that unique solutions exist and that the value of the critical coupling is in good agreement with both the analytical and numerical values found for the continuous analog of the DNLS. For the full system of equations, we believe that a large number of solutions exist for each choice of the coupling constants and that a conserved quantity exists in the system. The critical value of the electron-phonon coupling is of the same order of magnitude as in the case of the DNLS; however, we believe that this small discrepancy results from the fact that possible ''boundary'' terms appear when replacing the full system by the DNLS. These boundary terms are that which are annihilated by either the four-point Laplacian $\Delta(1)$ and/or by the seven-point Laplacian $\Delta(2)$. To find these terms is nontrivial and since this seems an interesting topic by itself, we leave this as a future work.[13]

Finally let us mention that a possible extension of the results given here would involve the study of the corresponding three-dimensional equations and/or of the influence of external forces.

APPENDIX: HAMILTONIAN AND EQUATIONS OF MOTION FOR THE NUMERICAL STUDIES

To simplify the numerical construction of the solutions we have squeezed the lattice as indicated in Figs. 2(a) and 2(b). This reduces the memory requirements and so speeds up the calculations. The Hamiltonian H^n for the numerical construction thus takes the form

$$H^n = \sum_{j=1}^{N_2} \sum_{(i-1)/4=0}^{(N_1/4)-3} \Bigg[(E+W)\psi_{i,j}\psi_{i,j}^* - j_x \psi_{i,j}^*(\psi_{i+1,j} + \psi_{i-1,j} + \psi_{i+1,j-1})$$

$$- j_x \psi_{i,j}(\psi_{i+1,j}^* + \psi_{i-1,j}^* + \psi_{i+1,j-1}^*) + \psi_{i,j}\psi_{i,j}^*\left(\frac{c_x}{3}(u_{i+1,j} + u_{i+1,j-1} - 2u_{i-1,j}) - \frac{c_x}{\sqrt{3}}(v_{i+1,j-1} - v_{i+1,j})\right)\Bigg]$$

$$+ \sum_{j=1}^{N_2} \sum_{(i-2)/4=0}^{(N_1/4)-2} \Bigg[(E+W)\psi_{i,j}\psi_{i,j}^* - j_x \psi_{i,j}^*(\psi_{i+1,j} + \psi_{i-1,j} + \psi_{i-1,j+1})$$

$$- j_x \psi_{i,j}(\psi_{i+1,j}^* + \psi_{i-1,j}^* + \psi_{i-1,j+1}^*) + \psi_{i,j}\psi_{i,j}^*\left(\frac{c_x}{3}(-u_{i-1,j} - u_{i-1,j+1} + 2u_{i+1,j}) + \frac{c_x}{\sqrt{3}}(v_{i-1,j+1} - v_{i-1,j})\right)\Bigg]$$

$$+ \sum_{j=1}^{N_2} \sum_{(i-3)/4=0}^{(N_1/4)-1} \Bigg[(E+W)\psi_{i,j}\psi_{i,j}^* - j_x \psi_{i,j}^*(\psi_{i+1,j} + \psi_{i-1,j} + \psi_{i+1,j+1}) - j_x \psi_{i,j}(\psi_{i+1,j}^* + \psi_{i-1,j}^* + \psi_{i+1,j+1}^*)$$

$$+ \psi_{i,j}\psi_{i,j}^*\left(\frac{c_x}{3}(u_{i+1,j} + u_{i+1,j+1} - 2u_{i-1,j}) + \frac{c_x}{\sqrt{3}}(v_{i+1,j+1} - v_{i+1,j})\right)\Bigg]$$

$$+ \sum_{j=1}^{N_2} \sum_{i/4=1}^{N_1/4} \Bigg[(E+W)\psi_{i,j}\psi_{i,j}^* - j_x \psi_{i,j}^*(\psi_{i+1,j} + \psi_{i-1,j} + \psi_{i-1,j-1}) - j_x \psi_{i,j}(\psi_{i+1,j}^* + \psi_{i-1,j}^* + \psi_{i-1,j-1}^*)$$

$$+ \psi_{i,j}\psi_{i,j}^*\left(\frac{c_x}{3}(u_{i-1,j} + u_{i-1,j-1} - 2u_{i+1,j}) + \frac{c_x}{\sqrt{3}}(v_{i-1,j} - v_{i-1,j-1})\right)\Bigg] \tag{A1}$$

with the phonon energy W^n,

$$W^n = \frac{1}{2}M \sum_{j=1}^{N_2} \sum_{i=1}^{N_1} \left(\left(\frac{du}{dt}\right)^2 + \left(\frac{dv}{dt}\right)^2 + k_x[(u_{ij} - u_{i-1,j})^2 + (v_{ij} - v_{i-1,j})^2]\right) + \frac{1}{2}M \sum_{j=1}^{N_2} \sum_{(i-2)/4=0}^{(N_1/4)-2} (k_x[(u_{ij} - u_{i-1,j+1})^2$$

$$+ (v_{ij} - v_{i-1,j+1})^2]) + \frac{1}{2}M \sum_{j=1}^{N_2} \sum_{(i-3)/4=0}^{(N_1/4)-1} (k_x[(u_{ij} - u_{i+1,j+1})^2 + (v_{ij} - v_{i+1,j+1})^2]). \tag{A2}$$

The equations of motion are then given by
For $i=1+4k$, $k=1,2,\ldots,$

$$i\hbar \frac{\partial \psi_{i,j}}{\partial t} = (E+W)\psi_{i,j} - 2j_x(\psi_{i+1,j} + \psi_{i-1,j} + \psi_{i+1,j-1})$$

$$+ \psi_{i,j}\Bigg[\frac{c_x}{3}(u_{i+1,j} + u_{i+1,j-1} - 2u_{i-1,j})$$

$$+ \frac{c_x}{\sqrt{3}}(v_{i+1,j} - v_{i+1,j-1})\Bigg], \tag{A3}$$

$$\frac{d^2 u_{i,j}}{dt^2} = -k_x(3u_{i,j} - u_{i+1,j} - u_{i-1,j} - u_{i+1,j-1})$$

$$- \frac{c_x}{3M}(2\psi_{i-1,j}\psi_{i-1,j}^* - \psi_{i+1,j}\psi_{i+1,j}^*$$

$$- \psi_{i+1,j-1}\psi_{i+1,j-1}^*), \tag{A4}$$

$$\frac{d^2 v_{i,j}}{dt^2} = -k_x(3v_{i,j} - v_{i+1,j} - v_{i-1,j} - v_{i+1,j-1})$$

$$- \frac{c_x}{\sqrt{3}M}(\psi_{i+1,j-1}\psi_{i+1,j-1}^* - \psi_{i+1,j}\psi_{i+1,j}^*). \tag{A5}$$

For $i=2+4k$, $k=1,2,\ldots,$

$$i\hbar \frac{\partial \psi_{i,j}}{\partial t} = (E+W)\psi_{i,j} - 2j_x(\psi_{i+1,j} + \psi_{i-1,j} + \psi_{i-1,j+1})$$

$$+ \psi_{i,j}\Bigg[\frac{c_x}{3}(-u_{i-1,j} - u_{i-1,j+1} + 2u_{i+1,j})$$

$$+ \frac{c_x}{\sqrt{3}}(v_{i-1,j+1} - v_{i-1,j})\Bigg], \tag{A6}$$

$$\frac{d^2 u_{i,j}}{dt^2} = -k_x(3u_{i,j} - u_{i+1,j} - u_{i-1,j} - u_{i-1,j+1})$$
$$+ \frac{c_x}{3M}(2\psi_{i+1,j}\psi^*_{i+1,j} - \psi_{i-1,j}\psi^*_{i-1,j}$$
$$- \psi_{i-1,j+1}\psi^*_{i-1,j+1}), \tag{A7}$$

$$\frac{d^2 v_{i,j}}{dt^2} = -k_x(3v_{i,j} - v_{i+1,j} - v_{i-1,j} - v_{i-1,j+1})$$
$$+ \frac{c_x}{\sqrt{3}M}(\psi_{i-1,j+1}\psi^*_{i-1,j+1} - \psi_{i-1,j}\psi^*_{i-1,j}). \tag{A8}$$

For $i = 3 + 4k$, $k = 1, 2, \ldots$,

$$i\hbar \frac{\partial \psi_{i,j}}{\partial t} = (E + W)\psi_{i,j} - 2j_x(\psi_{i+1,j} + \psi_{i-1,j} + \psi_{i+1,j+1})$$
$$+ \psi_{i,j}\left[\frac{c_x}{3}(u_{i+1,j} + u_{i+1,j+1} - 2u_{i-1,j}) \right.$$
$$\left. + \frac{c_x}{\sqrt{3}}(v_{i+1,j+1} - v_{i+1,j}) \right], \tag{A9}$$

$$\frac{d^2 u_{i,j}}{dt^2} = -k_x(3u_{i,j} - u_{i+1,j} - u_{i-1,j} - u_{i+1,j+1})$$
$$- \frac{c_x}{3M}(2\psi_{i-1,j}\psi^*_{i-1,j} - \psi_{i+1,j}\psi^*_{i+1,j}$$
$$- \psi_{i+1,j+1}\psi^*_{i+1,j+1}), \tag{A10}$$

$$\frac{d^2 v_{i,j}}{dt^2} = -k_x(3v_{i,j} - v_{i+1,j} - v_{i-1,j} - v_{i+1,j+1})$$
$$- \frac{c_x}{\sqrt{3}M}(\psi_{i+1,j}\psi^*_{i+1,j} - \psi_{i+1,j+1}\psi^*_{i+1,j+1}). \tag{A11}$$

For $i = 4 + 4k$, $k = 1, 2, \ldots$,

$$i\hbar \frac{\partial \psi_{i,j}}{\partial t} = (E + W)\psi_{i,j} - 2j_x(\psi_{i+1,j} + \psi_{i-1,j} + \psi_{i-1,j-1})$$
$$- \psi_{i,j}\left[\frac{c_x}{3}(u_{i-1,j} + u_{i-1,j-1} - 2u_{i+1,j}) \right.$$
$$\left. - \frac{c_x}{\sqrt{3}}(v_{i-1,j} - v_{i-1,j-1}) \right], \tag{A12}$$

$$\frac{d^2 u_{i,j}}{dt^2} = -k_x(3u_{i,j} - u_{i+1,j} - u_{i-1,j} - u_{i-1,j-1})$$
$$+ \frac{c_x}{3M}(2\psi_{i+1,j}\psi^*_{i+1,j} - \psi_{i-1,j}\psi^*_{i-1,j}$$
$$- \psi_{i-1,j-1}\psi^*_{i-1,j-1}), \tag{A13}$$

$$\frac{d^2 v_{i,j}}{dt^2} = -k_x(3v_{i,j} - v_{i+1,j} - v_{i-1,j} - v_{i-1,j-1})$$
$$+ \frac{c_x}{\sqrt{3}M}(\psi_{i-1,j}\psi^*_{i-1,j} - \psi_{i-1,j-1}\psi^*_{i-1,j-1}). \tag{A14}$$

*Email address: Betti.Hartmann@durham.ac.uk

†Email address: W.J.Zakrzewski@durham.ac.uk

[1] S. Iijima, Nature (London) **354**, 56 (1991).

[2] See, e.g., M.S. Dresselhaus, G. Dresselhaus, and P. Eklund, *The Science of Fullerenes and Carbon Nanotubes* (Academic, New York, 1996); *Carbon Nanotubes, Preparation and Properties*, edited by T.W. Ebbesen (CRC, Boca Raton, FL, 1996); R. Saito, G. Dresselhaus, and M.S. Dresselhaus, *Physical Properties of Carbon Nanotubes* (World Scientific, Singapore, 1998); P.J.F. Harris, *Carbon Nanotubes and Related Structures* (Cambridge University Press, Cambridge, 1999); *Carbon Nanotubes: Synthesis, Structure, Properties, and Applications*, edited by M.S. Dresselhaus, G. Dresselhaus, and P. Avouris (Springer-Verlag, Berlin, 2000).

[3] M.S.C. Mazzoni and H. Chacham, Phys. Rev. B **61**, 7312 (2000); L. Yang, M.P. Anantram, J. Han, and J.P. Lu, *ibid.* **60**, 13 874 (1999); C.-J. Park, Y.-H. Kim, and K.J. Chang, *ibid.* **60**, 10 656 (1999); M.S.C. Mazzoni and H. Chacham, Appl. Phys. Lett. **76**, 1561 (2000); M. Verissimo-Alves, R.B. Capaz, B. Koiller, E. Artacho, and H. Chacham, Phys. Rev. Lett. **86**, 3372 (2001).

[4] A.S. Davydov, *Solitons in Molecular Systems* (Reidel, Dordrecht, 1985).

[5] A. Scott, Phys. Rep. **217**, 1 (1992); *Nonlinear Excitations in Biomolecules*, edited by M. Peyrard (Springer, Berlin, 1996).

[6] L. Brizhik, A. Eremko, B. Piette, and W.J. Zakrzewski, Physica D **146**, 275 (2000).

[7] L. Brizhik, B. Piette, and W.J. Zakrzewski, Ukr. Fiz. Zh. **46**, 503 (2001).

[8] L. Brizhik, A. Eremko, B. Piette, and W.J. Zakrzewski, Physica D **159**, 71 (2001).

[9] L. Liu, G.Y. Guo, C.S. Jayanthi, and S.Y. Wu, Phys. Rev. Lett. **88**, 217206 (2002).

[10] U. Asher, J. Christiansen, and R.D. Russell, Math. Comput. **33**, 659 (1979); U. Asher, J. Christiansen, and R.D. Russell, ACM Trans. Math. Softw. **7**, 209 (1981).

[11] S. Coleman, Nucl. Phys. B **262**, 263 (1985); for a review, see, e.g., T.D. Lee and Y. Pang, Phys. Rep. **221**, 251 (1992).

[12] T. Spires and R.M. Brown, *High Resolution TEM Observations of Single-Walled Carbon Nanotubes*, Jr. Department of Botany, The University of Texas at Austin, Austin, Texas, 1996, see http://www.botany.utexas.edu/facstaff/facpages /mbrown/ongres/ tspires/nano.htm; J.W.G. Wilder, L.C. Venema, A.G. Rinzler, R.E. Smalley, and C. Dekker, Nature (London) **391**, 59 (1998).

[13] B. Hartmann and W.J. Zakrzewski (unpublished).